SUPPLEMENTARY INFORMATION

Supplementary Materials and Methods

Analysis of protein purity and oligomerization state

A Shimadzu LC20 HPLC (Kyoto, Japan) connected to Dawn Heleos II light scattering detector and Optilab reX refractometer (Wyatt Technologies Inc., CA) was used to combine size-exclusion chromatography with multi-angle laser light scattering measurements (SEC-MALS). SEC-MALS was used to analyze the purity and oligomeric state of proteins (Fig. S6). 100 μl samples were injected onto an analytical Superdex 75 SEC column (GE Healthcare, PA) equilibrated at 293 K with the following buffers: 10 mM sodium phosphate pH 7.4 (cytochrome b_{562}); 20 mM MOPS pH 7.0 (WW domain); 50 mM MES pH 6.3 (CI2, SOD1); 20 mM sodium acetate pH 5.2 (lysozyme); 50 mM sodium phosphate pH 7.0 (α-spectrin domains); 20 mM Tris pH 7.5 (PDZ1 F95W). The ionic strength of buffers was adjusted to 150 mM using sodium chloride (except for the α-spectrin and PDZ buffers). Astra software (Wyatt Technologies, CA) was used to analyze light scattering experiments.

Differential Scanning Calorimetry

The P60A mutant of R16 α-spectrin domain was studied using differential scanning calorimetry (DSC) and a Microcal capillary DSC (GE, PA). The protein was first dialyzed overnight into 50 mM sodium phosphate buffer pH 7.0 containing 0.05 % (*w*/*v*) sodium azide. Measurements were made at protein concentrations between 10 to 105 μM (and scan rates of 60-125 K/h). We found no evidence of a dependence on protein concentration or scan-rates. Protein denaturation was highly reversible on rescanning (despite heating to 378 K, Fig. S5). DSC data were fitted using Origin (OriginLab, MA).

Supplementary Figures

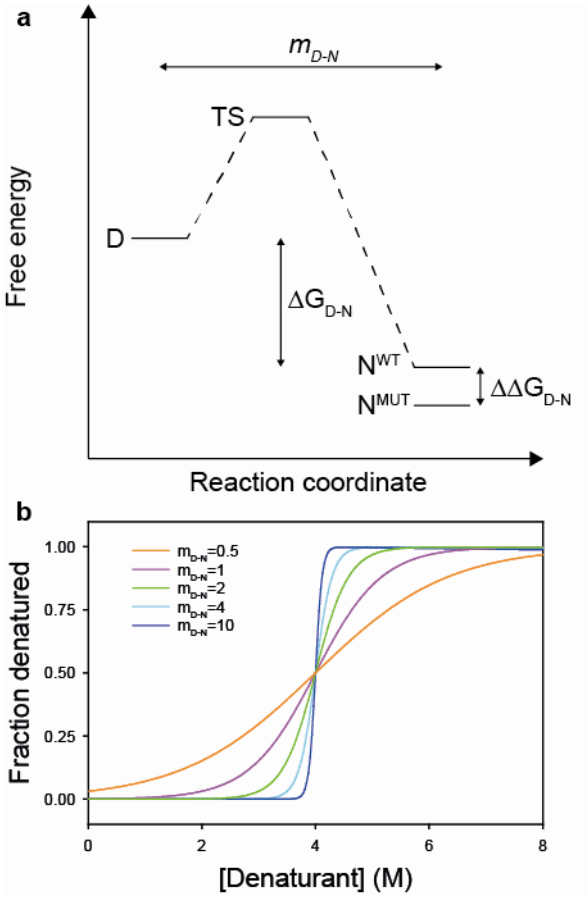

Supplementary Fig. S1 Basic thermodynamics of 2-state protein denaturation (a) Energy diagram and thermodynamic parameters associated with 2-state protein denaturation. Under conditions that favour folding, the denatured state (D) has a higher free energy than the native state (N) such that the latter preferentially accumulates. A protein's stability can be defined as the difference in free energy between these two states (ΔG_{D-N}). The progress along the reaction coordinate between N and D can be empirically related to the change in solvent accessible surface area associated with folding, which correlates with its $m_{\text{D-N}}$ value. The transition state (TS) is the highest energy species separating the N and D ensembles and is rate-limiting to folding and unfolding reactions. The stability change upon mutation of a protein ($\Delta\Delta G_{D-N}$) is quantified as the difference in free energy of denaturation for the mutant protein (N^{MUT}) relative to the wild type (N^{WT}) [1]. **(b)** The effect of $m_{D\text{-}N}$ on chemical denaturant titrations. All lines show a 2-state transition where $m_{D\text{-}N}$ varies from 0.5-10 kcal/mol.M. High $m_{\text{D-N}}$ values (typical of large proteins) yield narrow transitions with well-defined native and denatured baselines. Low $m_{\text{D-N}}$ values, typical of smaller proteins, have wide transitions but N and D baselines are poorly defined (see Fig. 1 in the *Main Text*) [1, 2].

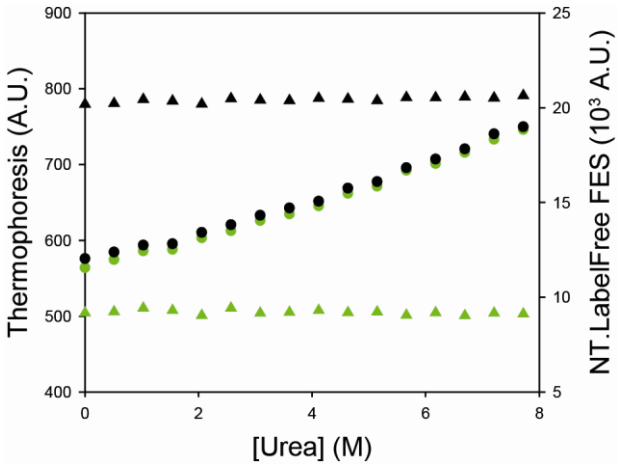

Supplementary Fig. S2 Effects of denaturant on tryptophan fluorescence emission and peptide thermophoresis. Titrating urea into a short, unstructured peptide (AWPAK) showed only a linear change in initial intrinsic fluorescence ("NT.LabelFree FES", circles) and peptide thermophoresis (triangles). This observation held true when ~2 K (black) or ~6 K (green) thermal gradients were used. Thus, the sigmoidal titration curves we present for proteins denaturation (see Fig. 3 in the *Main Text*) likely report on structural changes, not artefacts related to local fluorophore events or solvent viscosity. The observed linear change in fluorescence is consistent with known urea effects on tryptophan fluorescence emission [3].

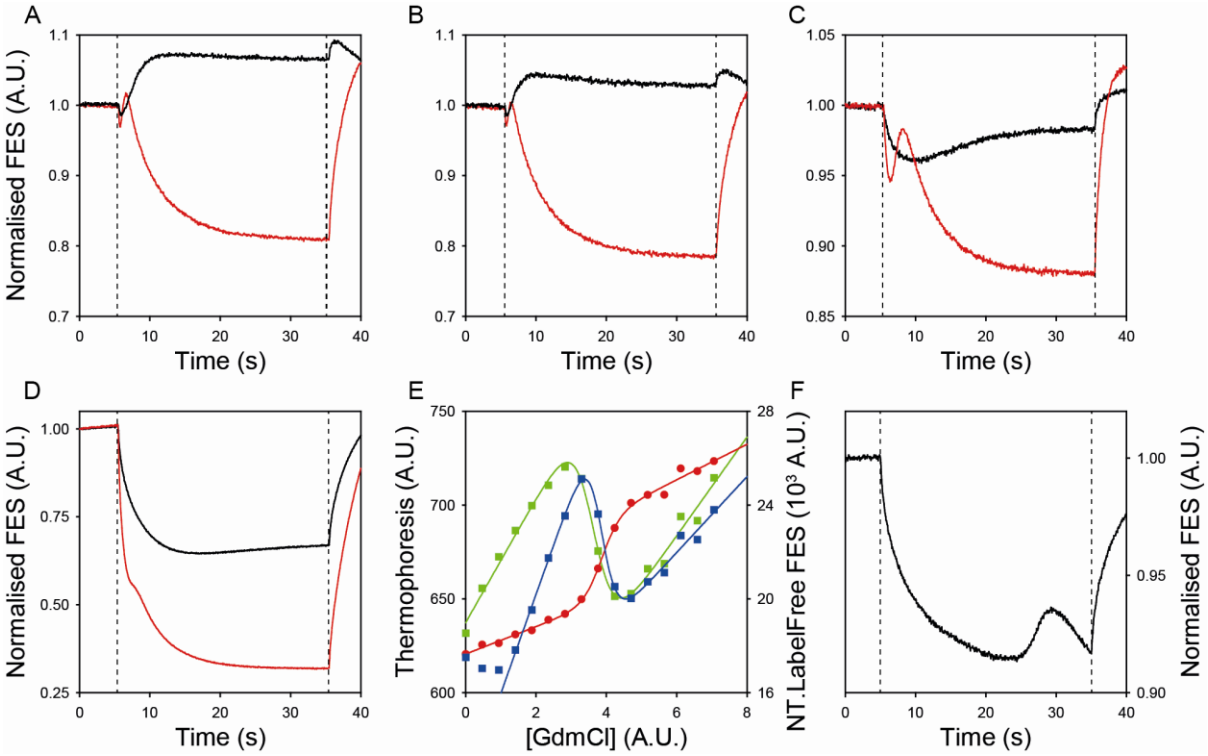

Supplementary Fig. S3 Examples of complex thermophoresis data associated with protein denaturation. **(a)** Wild type R16 in 2.6 M urea had non-exponential thermophoresis traces in ~2 K (black, 20% laser power) and ~6 K (red, 80% laser power) gradients. This behaviour was highly reproducible and not caused by protein aggregation. Dashed lines show when the laser was switched on and off. **(b)** We hypothesized these effects could be due to slower *cis-trans* proline isomerisation events. However, similar traces were observed for the P60A mutant of R16 α-spectrin (which has no proline residues). Further, no anomalies were observed for the AWPAK peptide (Fig. S3), which has temperature-dependent changes in proline isomerisation [4]. **(c)** Non-exponential traces were also seen for CI2 in 1.1 M GdmCl. **(d)** Non-exponential traces for lysozyme in 3.3 M GdmCl. The colors and symbols in (**b-d**) match those in (**a**). **(e)** Chemical denaturation of lysozyme. Denaturation was probed by fluorescence emission (red circles, "NT.LabelFree FES"), or thermophoresis (squares) with ~2 K (blue) or ~3 K (green) gradients. The large changes in fluorescence made robust definition of thermophoresis changes challenging. We also observed steep or non-linear baselines in titrations of other proteins (which arose from non-exponential kinetic traces). **(f)** Thermophoresis traces of HBc in 0.3 M GdmCl (using a 2 K gradient) [5]. The deviations observed were stochastic and different to the reproducible kinetics shown in (**a-d**). The HBc deviations were caused by convection moving MDa capsid-like particles (that HBc forms under these conditions) through the nanoliter detection volume of the instrument [5].

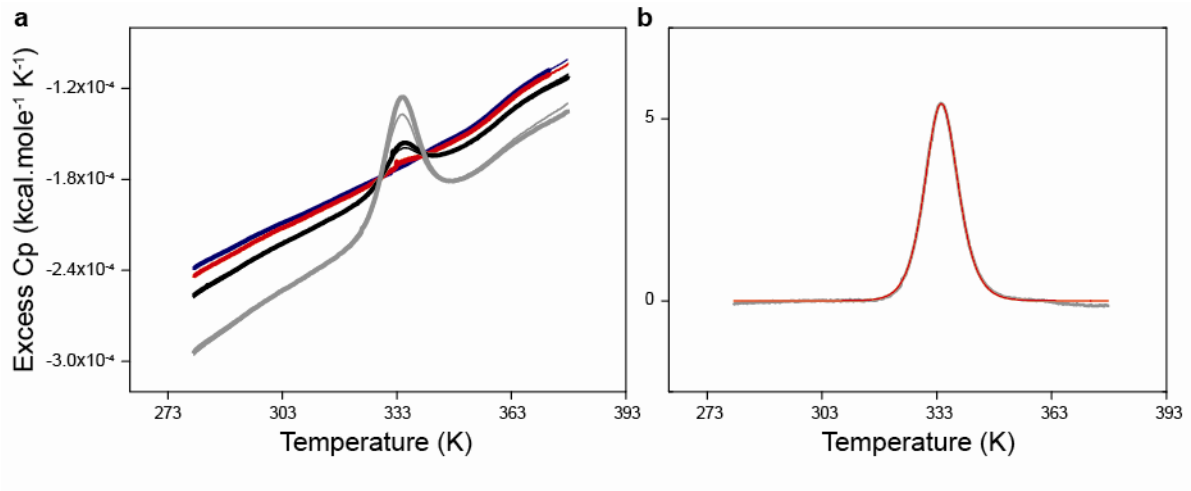

Supplementary Fig. S4 Thermal denaturation of the P60A mutant of the R16 α-spectrin domain measured by DSC. (a) Raw DSC data of the P60A mutant of the R16 α-spectrin domain measured at concentrations of 105 μM (grey), 30 μM (black) and 10 μM (red) using a scan rate of 60 K/h (see *Supplementary Information Materials and Methods*). Rescans of these samples are shown as thinner lines. The average of four different buffer baseline scans is shown (purple). **(b)** DSC data for the P60A mutant of the R16 α-spectrin domain after subtraction of the buffer baseline, concentration normalisation and subtraction of the intrinsic baseline between the native and denatured heat capacities (grey). The fit to a simple non-two state model (red) for the 105 μM data set, which had the best signal to noise ratio, yielded T_m and $\Delta H_{D\text{-}N}$ values of 344.6±0.1 K and 79.8±0.1 kcal/mol, respectively.

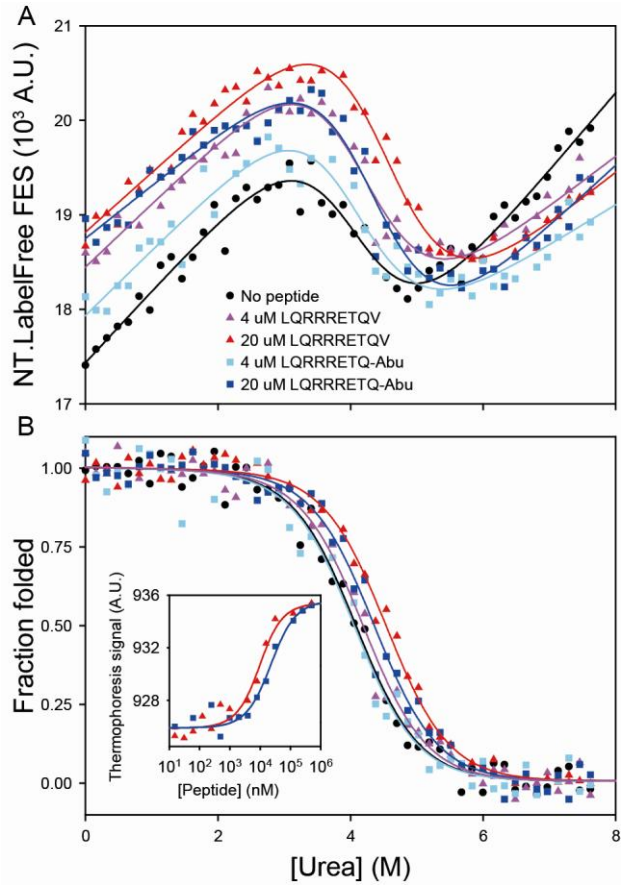

Supplementary Fig. S5 Denaturant titrations of PDZ1 F95W in the presence or absence of peptide ligands at 310 K. (a) Titrations of PDZ1 F95W in the absence (black circles) or presence of LQRRRETQV (triangles) or LQRRRETQ-Abu (squares) peptides measured using an NT.LabelFree at 310 K and peptide concentrations of 4 μM or 20 μM. Measuring these data at 310 K allowed baselines to be better defined than experiments performed at 298 K (Fig. 5*C* in the main text). The steep baselines observed are characteristic of PDZ1 F95W since the engineered tryptophan residue has a poor signal change upon denaturation (compared to the urea-dependence of native and denatured baselines). **(b)** Normalizing the data in (**a**) to fraction folded allowed the stability changes induced by peptide binding to be more clearly visualized (colours and symbols as per (**a**)). *Inset* The NT.Labelfree instrument was also used to perform MST-based binding titrations at 310 K for LQRRRETQV (red triangles) and LQRRRETQ-Abu (blue squares). These experiments defined apparent K_d values of ~7.1±0.5 μM and ~20±2 μM, respectively. The stability changes observed at 310 K were consistent with weaker K_d values at 310 K (compared to 298 K, Fig. 5*C*, *Main Text*). Nonetheless, the stability changes induced by 20 μM peptide was significant for both peptides ($\Delta[\text{Denaturant}]_{50\%}$ = 0.45±0.12 and 0.28±0.12 M respectively), with the stronger binder (LQRRRETQV) having a larger stability increase than the weaker binder (LQRRRETQ-Abu). Here we assume $\Delta[\text{Denaturant}]_{50\%}$ values of >0.1 M as significant, which is much stricter than widely accepted norms for denaturant titrations [6]. The beauty of our approach is that the magnitude of $\Delta[\text{Denaturant}]_{50\%}$ values can be tuned by varying the temperature and ligand concentration (compare Fig. S5a and Fig. 6b, Main Text). This allows the assay conditions to be tuned until the magnitude of ligand-induced changes in stability best fit ones requirements.

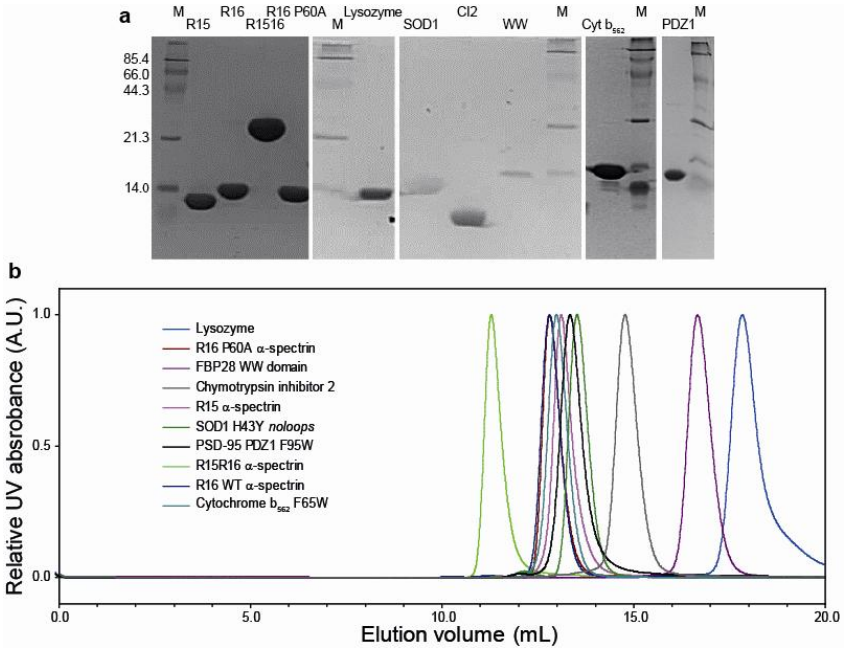

Supplementary Fig. S6 Confirming the purity and oligomeric state of proteins. (a) SDS-PAGE gel analysis of proteins used in this study. The molecular weight standards (lanes marked M) have their masses in (kDa) shown at left side of the gels. Labels above each lane identify each protein: "R15", "R16", "R1516" and "R16 P60A" denote the α-spectrin domain constructs; "lysozyme" denotes hen egg white lysozyme; "SOD1" denotes superoxide dismutase H43Y; "CI2" denotes wild type barley chymotrypsin inhibitor 2; "WW" denotes the murine FBP28 WW domain; "Cyt b_{562}" denotes the F65W mutant of *E. coli* cytochrome b_{562}; "PDZ1" denotes the F95W mutant of the first PDZ domain repeat of post-synaptic density protein 95. **(b)** Proteins were confirmed to be monomeric and >98 % pure by SEC-MALS analyses. The masses of proteins eluting from the SEC column were calculated from the angular dependence and intensity of scattered light (see *Supplementary Information Materials and Methods*).

Supplementary Table S1

Experimental parameters used for denaturant titrations

Protein	[Protein] (μM)	Size (kDa)	Fold	Buffer	Chaotrope	MST LED power
Lysozyme	10	14.3	αβ	20 mM sodium acetate pH 5.2	GdmCl	1
Cyt b_{562}	5	14.1	α	20 mM sodium phosphate pH 7.0, 57 mM NaCl	Urea	10
CI2 [a]	5	7.3	αβ	50 mM MES pH 6.3	GdmCl	20
WW	2	4.5	β	20 mM MOPS pH 7.0, 150 mM Na_2SO_4	GdmCl	25
R15	4	13.1	α	50 mM sodium phosphate pH 7.0	Urea	15
R16	2	13.8	α	50 mM sodium phosphate pH 7.0	Urea	22
R16 P60A	2	13.8	α	50 mM sodium phosphate pH 7.0	Urea	25
R1516	2	25.8	α	50 mM sodium phosphate pH 7.0	Urea	15
SOD1	4	11	β	10 mM MES pH 6.3	Urea	30
AWPAK	53	0.6	N/A	50 mM sodium phosphate pH 7.0	Urea	7
PDZ1	5	10.5	αβ	50 mM Tris.HCl, 157 mM NaCl, 10 mM $MgCl_2$, 0.05% TWEEN, pH 7.5	Urea	15 [b]

Protein names denoted as in Fig. S6*A*.

[a] CI2 was measured on the AB2 fluorimeter using a protein concentration of 2.5 μM.

[b] An LED power of 20 % was used at 310 K to compensate for attenuation of the fluorescence signal at this temperature.

Supplementary Table S2 Comparison between some commonly used techniques for measuring protein-ligand interactions and our capillary-based denaturant titration approach

	ITC [7, 8]	DSF [9,10]	SPR [11-13]	MST [14]	Capillary-based denaturant titrations
Probes	Heat evolved or released on binding	Changes in T_m values	Dipole changes near a gold chip surface	Solvation shell changes	Increases in $[Den]_{50\%}$ values
Protein sample consumed per measurement	Up to 2 mg per measurement	2 µg per well	~100 µg per screen	1-3 µg (LabelFree) 10-50 ng (NT.115[a])	5-10 µg titration
No. of measurements per day[b]	3 (Manual ITC) ~25 (Robotic ITC)	Up to 7000 interactions	~72 × 6-point dose-response titrations	720 titrations[c]	576 titrations[d]
Typical maximum [ligand]	10 to 100-fold × K_d	1 to 10-fold × K_d	10 to 100-fold × K_d	10 to 100-fold × K_d	1 to 10-fold × K_d
Volume per measurement	~100 µl	5-20 µl	~200 µl	60-200 µl	0.2-0.5 ml
Sample limitations	Buffers need to be carefully matched to avoid false-positives	Must not aggregate at elevated temperatures	Protein needs to be immobilised to surface layer on SPR chips	Ligand must not fluoresce at the wavelengths used to probe MST	Ligand must not fluoresce at same wavelengths as used to probe MST
Automation	Possible with auto-titrators but these have relatively low throughput (≤25 interactions/day)	Automation possible in 96- and 384-well microplate formats	Using multiplex SPR instruments, up to 36 interactions/experiment can be measured	Up to 96 samples can be measured simultaneously (on an NT.Automated)	Up to 96-samples can be measured simultaneously (on an NT.Automated)
Additional comments	Binding K_d, enthalpy, entropy and stoichiometries determined in a single experiment	Typically requires the use of molecular probes	Immobilisation can inhibit or perturb binding. K_d and binding kinetics can be determined.	Protein aggregates visible in MST time traces. K_d-values can be determined.	Urea the preferred denaturant as it is non-ionic and shouldn't screen out electrostatic interactions.

[a] The Monolith.NT.115 can measure MST for protein targets extrinsically labelled with fluorescent dyes (that have a range of different coupling chemistries and quantum yields)

[b] Interaction measurements made per person per day per instrument

[c] Figure based on 16-point titrations and a NT.LabelFree Automated which can measure six 16-point titrations in ~15 minutes (see Main Text). Whilst this approach employs a lower data point density, it is acceptable for screening purposes.

[d] Figure based on 24-point titrations and a NT.LabelFree Automated which can measure four 24-point titrations in ~8 minutes (see Main Text). Whilst this approach employs a lower data point density, it is acceptable for screening purposes.

SUPPLEMENTARY REFERENCES

[1] Onuchic JN, Wolynes PG. Theory of protein folding. Curr. Opin. Struct. Biol. 2004;14:70-5

[2] Myers JK, Pace CN, Scholtz JM. Denaturant m values and heat capacity changes: relation to changes in accessible surface areas of protein unfolding. Prot. Sci. 1995;4:2138-48

[3] Joerger AC, Fersht AR. Structural biology of the tumor suppressor p53. Ann. Rev. Biochem. 2008;77:557-82

[4] Reimer U, Scherer G, Drewello M, Kruber S, Schutkowski M, Fischer G. Side-chain effects on peptidyl-prolyl *cis*/*trans* isomerisation. J. Mol. Biol. 1998;279:449-60

[5] Alexander CG, Jurgens MC, Shepherd DA, Freund SM, Ashcroft AE, Ferguson N. Thermodynamic origins of protein folding, allostery, and capsid formation in the human hepatitis B virus core protein. Proc. Natl. Acad. Sci. U S A. 2013;110:E2782-91

[6] S. Sato, T.L. Religa, A.R. Fersht, Phi-analysis of the folding of the B domain of protein A using multiple optical probes., J. Mol. Biol., 360 (2006) 850-864

[7] Freire E, Mayorga OL, Straume M. Isothermal titration calorimetry. Anal. Chem. 1990;62:950A-959A

[8] Natalia Markova Robjmkhmamwma. The advantages of Micro-Cal™ Auto-iTC200 for secondary screening in a fragment-based drug discovery campaign. The Association of Biomolecular Resource Facilities; 2013. p. S47-S

[9] Senisterra Ga, Soo Hong B, Park H-W, Vedadi M. Application of high-throughput isothermal denaturation to assess protein stability and screen for ligands. J. Biomol. Screen. 2008;13:337-42

[10] Capelle MaH, Gurny R, Arvinte T. High throughput screening of protein formulation stability: practical considerations. Eur. J. Pharm. Biopharm: Official Journal of Arbeitsgemeinschaft für Pharmazeutische Verfahrenstechnik eV. 2007;65:131-48

[11] Boozer C, Kim G, Cong S, Guan H, Londergan T. Looking towards label-free biomolecular interaction analysis in a high-throughput format: a review of new surface plasmon resonance technologies. Curr. Opin. Biotech. 2006, 17(4):400-5

[12] Abdiche YN, Lindquist KC, Pinkerton A, Pons J, Rajpal A. Expanding the ProteOn XPR36 biosensor into a 36-ligand array expedites protein interaction analysis. Anal. Biochem. 2011;411:139-51

[13] Bravman T, Bronner V, Lavie K, Notcovich A, Papalia GA, Myszka DG. Exploring "one-shot" kinetics and small molecule analysis using the ProteOn XPR36 array biosensor. Anal. Biochem. 2006;358:281-8

[14] Jerabek-Willemsen M, Wienken CJ, Braun D, Baaske P, Duhr S. Molecular interaction studies using microscale thermophoresis. Assay Drug. Dev. Technol. 2011;9:342-53